International Research Journal of Innovations in Engineering and Technology (IRJIET)

ISSN (online): 2581-3048

Volume 8, Issue 11, pp 122-127, November-2024

https://doi.org/10.47001/IRJIET/2024.811011

Fatigue and Damage Tolerance Analysis on Center Wing N-XXX Aircraft Using Software

[1]Djoeli Satrijo, [2]*Ojo Kurdi, [3]Toni Prahasto, [4]Sabrina Rizky Mulyana, [5]Ian Yulianti

[1,2,3,4]Mechanical Engineering, Faculty of Engineering, Diponegoro University, Jl. Prof. Sudharto, SH., Tembalang-Semarang 50275, Indonesia

[5]Physics Study Program, Universitas Negeri Semarang, Central Java, Indonesia

*Corresponding Author's E-mail: ojokurdi@ft.undip.ac.id

***Abstract* - The aircraft wing is the most important part of the aircraft which functions to provide a lift so that the aircraft can fly. The material structure of the aircraft wing will experience fatigue due to its condition in the air which requires elasticity to produce continuous movement. Therefore, fatigue and damage tolerance analysis were carried out. Fatigue analysis can determine the life of a component undergoing loading from an aircraft structure, while damage tolerance analysis can predict the rate of crack propagation and the residual life of structures that have been cracked. By combining these two analyses, the best management program for aircraft structures, especially aircraft wings, can be created. In this test, calculations and analysis were performed with software with the crack growth principle. In this study, the calculation results are still within the range that should be set by the company.**

Keywords: Aircraft Wing, Fatigue Analysis, Fracture Mechanic.

I. INTRODUCTION

Failures can occur for many reasons, such as environmental or loading uncertainties, material defects, design errors, and construction or maintenance deficiencies. Fracture design has its own technology and is currently the subject of very interesting research [1].For decades, it has been recognized that cracks or defects in a material reduce the strength of that material below the strength described by the strength of the material. This led to the establishment of residual strength as an important factor in the design of engineered components for safe service life, and the damage tolerance program in engineering was initiated. Hence, the discipline established to address the residual strength of cracked components focused on damage tolerance [2].

In some aircraft parts, maintenance and repair must be done as well as possible to keep the aircraft operating properly. Although making repairs requires knowledge of the forces or stresses that occur at some damaged locations as well as the forces or stresses at those locations after the repair to ensure that the repaired locations are better than before the repair, it is often necessary to add certain equipment both inside and outside the aircraft. To ensure that the installation of components on that part of the aircraft does not compromise its structure, a series of analyses must be performed. To repair and add components to an aircraft, a set of knowledge and understanding of the supporting software as well as analytical knowledge relevant to the case at hand is required [3].

The wing component of an airplane is very important as it serves to generate lift. In addition, an airplane wing is subjected to different pressures from the top and bottom sides as it works in a very extreme environment, including high pressure and temperature. However, as the aircraft wing collides with the air ahead, the temperature increases. Therefore, aircraft components must undergo material failure checks and analysis. In the structure, it is susceptible to fatigue of the material structure which can threaten the safety of passengers if a fracture occurs. This fracture occurs due to an initial crack in the structure that will continue to grow in line with the number of flights carried out. This initial crack usually occurs due to joints, holes, and nails or rivets. On the wing of the aircraft itself there is an assembled body between the structure or wing frame and the skin using rivets. Because of this, it is very vulnerable for the aircraft wing to experience cracks and fractures in its structure [4].

Although aircraft spectra are loaded from various sources, fatigue crack growth (FCG) is usually predicted using uniaxial load spectra in aircraft structural integrity management. As graphically depicted in Figure 1, an aircraft wing is subjected to a spectrum of shear loads and axial loads. The axial load comes from the bending of the wing box along the span, which mainly occurs during the dynamic landing and taxiing phases. Specifically, the axial and shear load changes occur almost simultaneously, and the number of axial cycles is greater than that of shear cycles [5].

ISSN (online): 2581-3048
Volume 8, Issue 11, pp 122-127, November-2024
https://doi.org/10.47001/IRJIET/2024.811011

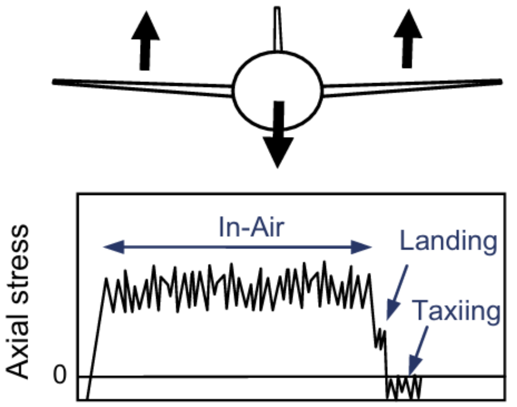

Figure 1: Axial load resulted from wing box span-wise bending [5]

Damage tolerance is an issue related to flight safety and is defined as a measure of the degree to which a component can perform its design function despite damage or defects. As a result, damaged parts must have sufficient residual strength and stiffness to continue operating safely during planned maintenance and inspection intervals. If damage occurs in critical areas that jeopardize flight safety, the component must be repaired or replaced to its full-service life or replaced completely. If damage is not detected, the machine must be able to operate safely until full-service life or a specified number of maintenance intervals after damage reaches a detectable level. To avoid the need for component replacement, a deeper understanding of the damage resistance of connected structures is required [6,7]

In recent years, there has been a growing focus on investigating the fatigue behavior and failure modes of various composite material structures. Fatigue is the deterioration of a material caused by fluctuating stresses that are smaller than the maximum tensile stress (ultimate tensile stress) and yield stress (yield stress) of the material given a constant load [8,9]. The stage of fatigue propagation is depicted in Figure 2.

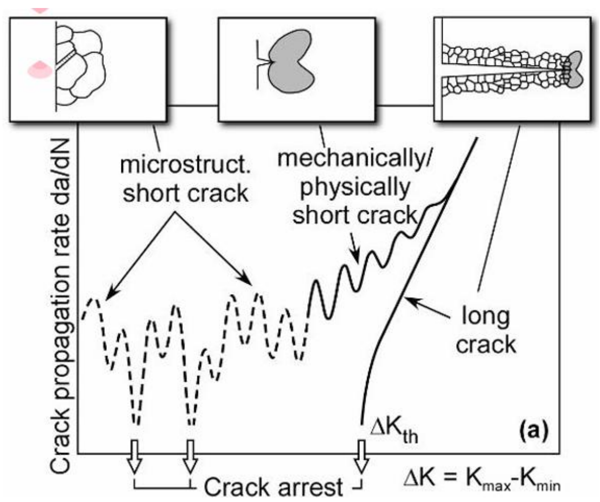

Figure 2: Stage of fatigue crack propagation [8]

Three phases comprise fatigue fracture: 1. Crack initiation, the fatigue mechanism usually starts with crack initiation at the weak surface of the material or at the place where there is stress concentration on the surface (such as notch, hole, scratch, etc.). 2. Crack propagation, crack initiation develops into microcracks, and the propagation or coalescence of these microcracks then forms macrocracks that will propagate. 3. Fracture, ooccurs when the material is subjected to stress and strain cycles that cause permanent damage [10].

Fracture is the final stage of the fatigue process where the material cannot withstand the existing stress and strain so that it breaks into two or more parts. In solid mechanics, the term "crack mechanics" refers to an important specialization in which cracks exist and the quantitative relationship between the length of the crack, the resistance of the material attached to the crack, and the stress at which the crack propagates at a high-speed leading to structural failure.To explain the state of cracks and their propagation within structures, fracture mechanical models have been created. This method was originally used for brittle materials [10,11,12].

The purpose of this study concerns the fracture phenomenon, which shows the analytical data of crack growth of the aircraft wing. So that the age and amount of residual stress of the structure can be known. This serves as a reference for the inspection and maintenance schedule of the aircraft wing.

II. RESEARCH METHODOLOGY

2.1 Data Collection Process

The data collection process involves several things, including:

a) Primary Structural Element: is a combination of components that form the basic framework of the aircraft and are responsible for the strength, rigidity and overall shape of the aircraft. These elements work together to withstand loads during flight, such as lift, drag and maneuvering loads. In the PSE, containing the geometry and size of its constituent components
b) Load and Stress: the load applied to the aircraft structure during testing is a repetitive load. The loads for calculating these stresses were taken from the detailed results of the finite element model showing the loads on the rear spar cap. Then the 1G, 1.5G, and boundary stresses are taken from these elements ID stresses.
The stresses transferred through the crack surfaces are also very complex, as the cracks shift between each other. The frequency and amplitude of the load are also very important. Frequency is the number of load cycles per unit

ISSN (online): 2581-3048
Volume 8, Issue 11, pp 122-127, November-2024
https://doi.org/10.47001/IRJIET/2024.811011

time, while amplitude is the magnitude of the maximum load applied. These two parameters will greatly affect the crack growth rate of the material [13].

c) Material Properties: is an intrinsic characteristic of a material that determines how it will interact with its environment and respond to different types of loads. The material properties can be influenced by plastic deformation. The material used for this part is Al 2024-T3 for spar cap and Al 2024-T351 for skin. Then from these material properties the mechanical static properties data is taken. The material properties as shown in Table 1 and Table 2 below [14].

Table 1: Mechanical Static Properties Al 2024-T3

Form and Specification	Clad Sheet QQ-A-250/5							
Temper	T3							
Thickness, mm	0.2-0.23		0.25-1.6		1.6-3.3		3.3-6.3	
Basis	A	B	A	B	A	B	A	B
Mechanical Properties								
σ_{tu}, MPa L	407	413	413	420	427	434	434	441
LT	400	407	407	413	420	427	427	434
ST								
σ_{ty}, MPa L	303	310	303	310	310	324	310	324
LT	269	276	269	276	276	289	276	289
ST								
σ_{cy}, MPa L	248	255	248	255	255	269	255	269
LT	289	296	289	296	296	310	296	310
ST								
τ_u , MPa	255	255	255	262	262	269	269	276
σ_{bru}^a, Mpa e/D=1.5	662	669	669	669	682	696	703	717
e/D =2.0	820	834	834	848	862	875	875	889
σ_{bry}^a, MPa e/D=1.5	469	482	469	482	482	503	482	503
e/D=2.0	565	579	565	579	579	607	579	607
Elongation, e% L								
LT	10		12-15		15		15	
ST								
μ, Elastic	0.33							
E, MPa Primary	72397							
Secondary	65502				68950			
Ec, MPa Primary	73776							
Secondary	66881				70329			
G, MPa								

Table 2: Mechanical Static Properties Al 2024-T351

Form and Specification	Bare Plate QQ-A-250/4											
Temper	T351											
Thickness, mm	6.3-12.7		12.7-24.4		24.4-38.1		38.1-50.8		50.8-76.2		76.2-101.6	
Basis	A	B	A	B	A	B	A	B	A	B	A	B
Mechanical Properties												
σ_{tu}, MPa L	441	455	434	448	427	441	427	441	413	427	393	407
LT	441	455	434	448	427	441	427	441	413	427	393	407
ST									358	372	338	351
σ_{ty}, MPa L	331	345	331	345	324	345	324	338	317	331	296	317
LT	289	303	269	303	289	303	289	303	289	303	282	296
ST									262	276	262	269
σ_{cy}, MPa L	269	282	269	282	269	276	262	276	255	269	241	255
LT	310	324	310	324	303	317	303	317	296	310	282	296
ST									317	331	303	324
τ_u , MPa	262	269	255	262	255	262	255	262	241	255	234	241
σ_{bru}^a, Mpa e/D=1.5	669	689	655	675	645	669	648	669	627	648	593	613
e/D=2.0	820	841	806	827	793	820	793	820	765	793	731	751
σ_{bry}^a, MPa e/D=1.5	496	524	496	524	496	524	496	524	496	524	482	510
e/D=2.0	593	620	593	620	593	620	593	620	593	620	579	607
Elongation, e% L												
LT	12		8		7		6		4		4	
ST												
μ, Elastic	0.33											
E, MPa Primary	73776											
Ec, MPa Primary	75155											
G, MPa	27580											

d) Flight Profile Spectrum: is a graphical or numerical representation of the load variations experienced by an aircraft structure during its flight cycle. This spectrum illustrates the load fluctuations that occur due to various flight conditions.

e) Finite Element Model (FEM): FEM was developed to determine the stress level and critical location of this PSE. In the process of updating the FE model, the laws of mechanics are used to create a structural model and the input load and unknown parameters are calculated by the measurement response [15].

f) Critical Location: in the PSE region is determined based on highest stress on the part and highest bearing force on the rivet hole in the high stress level zone. Picture 1 shows the results of the Critical location analysis located in the red section, where the area has the greatest stress among other areas of the structure.

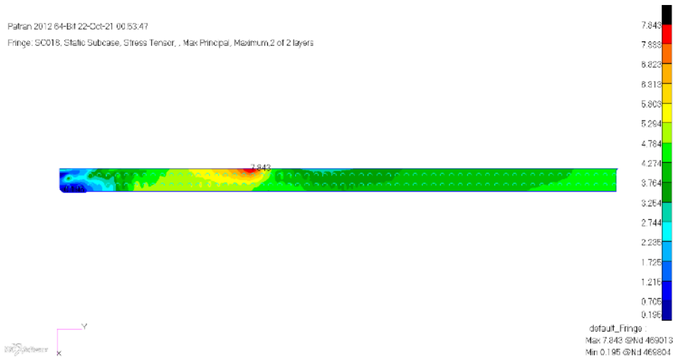

Figure 3: Result of finite element model of spar cap

On the spar cap, a corner crack with IMF (Initial Manufacture Flaw = 1.27 mm) grows from the fastener hole and then grows like a through-crack toward the near edge of the part. At the same time, on the opposite side of the hole, an angular crack with IQF (Initial Quality Flaw = 0.127 mm) developed to a through-crack. Subsequently, the crack grows as an edge crack towards the end of the part. While on the skin, the corner crack with IQF grows from the fastener hole and then grows as a through crack towards the near edge of the part. At the same time, on the opposite side of the hole, the corner crack with IQF grows to a through crack. And finally, the crack grows as an edge crack toward the end of the part.

g) Beta factor (β): is a provision of the program that states the form of propagation. This data become a parameter used in fatigue resistance analysis to take into account the effect of the geometric shape of a component on its fatigue strength. This factor is very important because the geometry of a component can significantly affect the stress distribution within the material, thereby affecting the crack initiation point and crack growth rate.

International Research Journal of Innovations in Engineering and Technology (IRJIET)

ISSN (online): 2581-3048

Volume 8, Issue 11, pp 122-127, November-2024

https://doi.org/10.47001/IRJIET/2024.811011

2.2 Calculation Process

The troubleshooting procedure in this process is carried out to analyze crack growth and predict the life of the specified structure. This calculation is carried out in stages in several subgroups or stages between four or five stages. This is done because it considers the shape of the crack growth and the length of the structure to get a more accurate value.

In the calculation process, there is a relationship with stress intensity. Stress intensity factor describes the stress conditions the crack tip and is related to the crack growth rate. Stress intensity factor is a function of the geometry, size, shape of the crack, and the type of load.

$$K = \sigma\sqrt{\pi a}\beta$$

where, Kisthestressintensityfactor, σ is the stress perpendicular to the crack propagation direction, a is the crack length, and β is the beta factor. The beta factor, whoes values will differ depending on the location and geometry.

III. RESULTS AND DISCUSSIONS

3.1 Geometry of Spar Cap and Skin Structure

The geometry of structure is shown in figure 4 below.

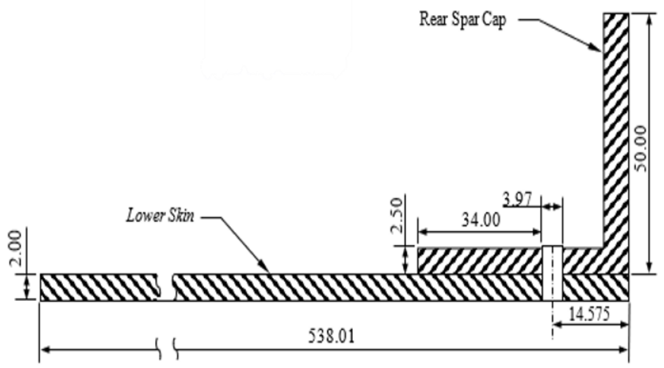

Figure 4: Geometry of Spar Cap and Skin

3.2 Calculation at Critical Location

In doing the calculation, there are 4 parts, each of which is divided into 3 to 4 right and left stages which represent the direction of propagation from the right and left sides of the rivet hole. The calculation always starts at the same number of flights. That is, at each stage if it starts from a different flight with a long range, then interpolation is performed.

In the crack growth test for the Spar Cap section, the results are shown in Table 3. The results in the calculation show that stage B or the right side of the hole experiences faster crack growth. This should not happen because the length of the stage b rod is more than the length of the stage A rod. However, due to the rivet hole connecting the Spar Cap to the skin, the stress on stage B is greater. This causes cracks to occur faster on the right side of the hole. Similarly to the Spar Cap, the skin also has higher stress on the right side of the hole than the left, resulting in stage B or the longer section having a higher crack speed. The results of crack growth calculations are shown in Table 4. Next is the calculation for the durability of Spar Cap and Skin. In contrast to crack growth, durability calculations are used to determine the timing of the first inspection of an aircraft. Then the maintenance schedule is determined from the results of the structural residual stress calculation. Table 5 shows the results of the durability calculation on the Spar Cap and Table 6 shows the results of the durability calculation on Skin. From the results shown, almost all parts of the structure will collapse before reaching the end of the structure. This shows the importance of regular maintenance even at the slightest crack growth.

Table 3: Crack growth for the Spar Cap

Stage		Input (mm)			β	a (mm)	flight
		a_0	a_{max}	b_0			
1	A	1,27	2,5	1,27	11;41; 46	1,657	171
	B					1,152	1425
2	A	1.657	32,015	1,27	12;15;41	32,015	15001
3	A	3,385	33,653		51;41	33,650	9143
	B	3,850				63,392	8537
4	A	81,726	97,151		2;41	83,799	8539

Table 4: Crack growth for the Skin

Stage		Input (mm)			β	a (mm)	flight
		a_0	a_{max}	b_0			
1	A	0,127	2,0	0,127	11;41;46	1,246	3373
	B					1,239	3318
2	A	3,228	14,257		51;41	14,250	17014
	B		523,752		52;41	260,275	14794
3	A	4,456	14,261		51;41;45	14,260	9264
	B		523,748			266,392	20139
4	A	24,249	538,008		2;41;45	326,626	23359

Table 5: Durability for the Spar Cap

Stage		Input (mm)			β	a (mm)	flight
		a_0	a_{max}	b_0			
1	A	0,254	2,5	0,254	11;41;46	1,519	1064
	B					1,515	918
2	A	3,502	33,998		51;41	33,998	9437
	B		63,153			63,059	8721
3	A	3,385	97,151		2;41	82,755	8723

International Research Journal of Innovations in Engineering and Technology (IRJIET)

ISSN (online): 2581-3048

Volume 8, Issue 11, pp 122-127, November-2024

https://doi.org/10.47001/IRJIET/2024.811011

Table 5: Durability for the Skin

Stage		Input (mm)			β	a (mm)	flight
		a_0	a_{max}	b_0			
1	A	0,254	2,0	0,254	11;41;46	1,236	2118
	B					1,237	2090
2	A	3,222	14,261		51;41	14,200	15825
	B		523,008		52;41	274,430	23602
3	A	4,456	538,008		2;41	320,957	18619

After performing the calculation, the entire output is processed to obtain a curve so that the curve can make it easier to determine the critical point and threshold inspection. The curves are shown in Figure 6, Figure 6, and Figure 7 below.

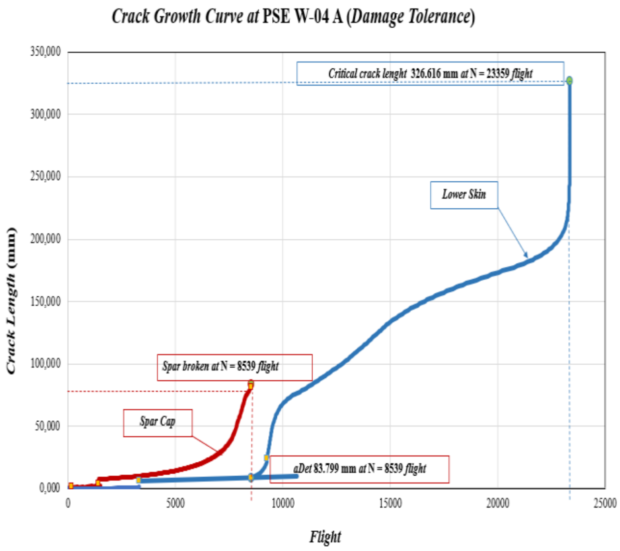

Figure 5: Crack growth damage tolerance graph

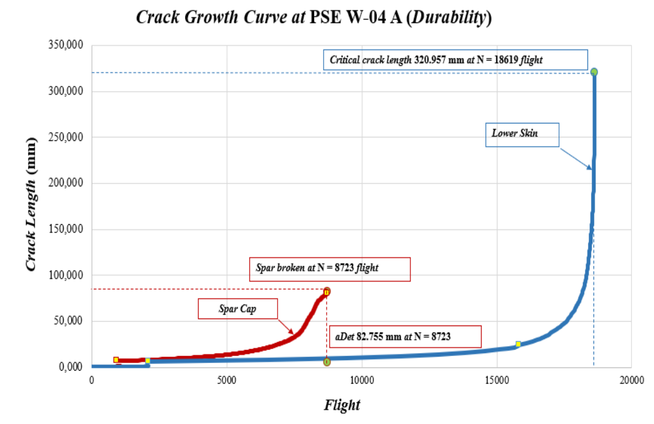

Figure 6: Crack growth durability graph

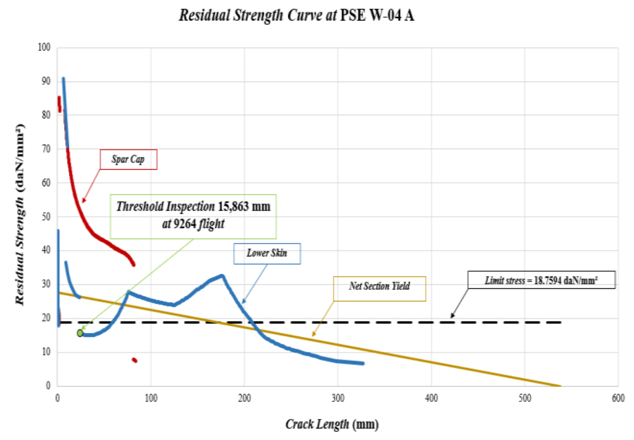

Figure 7: Residual Strength graph

IV. CONCLUSION

In this analysis, the author can draw several conclusions, from the calculations carried out, it is known that the critical crack length reaches 326.616 mm with a total of 23359 flights. For this reason, threshold inspection is carried out at 9264 flights and interval inspection at 14095 flights. This value is still in accordance with the range that recommended by standard.

REFERENCES

[1] Richard, H.A. and Sander, M. (2016) 'Fundamentals of fracture mechanics', *Solid Mechanics and its Applications*, 227(October), pp. 55–112. Available at: https://doi.org/10.1007/978-3-319-32534-7_3.

[2] Cano, A.J., Salazar, A. and Rodríguez, J. (2024) 'Structural integrity of polymers processed by additive manufacturing techniques using residual strength diagrams', *Theoretical and Applied Fracture Mechanics*, 134(PB), p. 104727. Available at: https://doi.org/10.1016/j.tafmec.2024.104727.

[3] Rita Zuana Qomariyah, S.Si, M.T. (2018) 'Dapat Memperbaiki Sistem Pemeliharaan Struktur Pesawat Udara', *Jurnal Pendiidkan*, 3(2), pp. 12–16.

[4] Karimah, A.L. *et al.* (2022) 'Analisis Kegagalan Material Pada Sayap Pesawat Terbang (Review)', *Jumantara Jurnal Manajemen dan Teknologi Rekayasa*, 1(1), p. 26. Available at: https://doi.org/10.28989/jumantara.v1i1.1266.

[5] Yu, X. (2014) 'On the fatigue crack growth analysis of spliced aircraft wing panels under sequential axial and shear loads', *Engineering Fracture Mechanics*, 123, pp. 116–125. Available at: https://doi.org/10.1016/j.engfracmech.2014.03.018

[6] Zerbst, U., Madia, M. and Vormwald, M. (2017) 'Fatigue strength and fracture mechanics', *Procedia*

ISSN (online): 2581-3048
Volume 8, Issue 11, pp 122-127, November-2024
https://doi.org/10.47001/IRJIET/2024.811011

Structural Integrity, 5, pp. 745–752. Available at: https://doi.org/10.1016/j.prostr.2017.07.165.

[7] Wei, Y. *et al.* (2024) 'On impact response and damage tolerance of adhesively bonded joints - An experimental and numerical study', *Thin-Walled Structures*, p. 112606. Available at: https://doi.org/10.1016/j.tws.2024.112606.

[8] Minigher, P. *et al.* (2024) 'On an efficient global/local stochastic methodology for accurate stress analysis, failure prediction and damage tolerance of laminated composites', *International Journal of Solids and Structures*, 303(January), p. 113026. Available at: https://doi.org/10.1016/j.ijsolstr.2024.113026

[9] Zhang, Y. *et al.* (2025) 'Predicting the fatigue life of T800 carbon fiber composite structural component based on fatigue experiments of unidirectional laminates', *International Journal of Fatigue*, 190(September 2024), p. 108622. Available at: https://doi.org/10.1016/j.ijfatigue.2024.108622.

[10] Randy Septiawan, dan (2018) 'Jurnal Rekayasa Material, Manufaktur dan Energi Analisa Pengujian Lelah Material Stainless Steel 304 Dengan Menggunakan Rotary Bending Fatigue Machine', *Jurnal Rekayasa Material, Manufaktur dan Energi*, 1(1), pp. 64–73. Available at: https://creativecommons.org/licenses/by-sa/4.0/

[11] Richard, H.A. and Sander, M. (2016) 'Fundamentals of fracture mechanics', *Solid Mechanics and its Applications*, 227(October), pp. 55–112. Available at: https://doi.org/10.1007/978-3-319-32534-7_3.

[12] Kolditz, L.M. *et al.* (2024) 'Employing Williams ' series for the identification of fracture mechanics parameters from phase-field simulations', *Engineering Fracture Mechanics*, 307(October 2023), p. 110298. Available at: https://doi.org/10.1016/j.engfracmech.2024.110298.

[13] Boutelidja, R. *et al.* (2024) 'A dual fracture mechanical approach for estimating notch stress intensity factor and T-stress using volumetric methods on API 5L pipe steel: Experimental study and numerical validation', *Journal of Materials Research and Technology*, 33(October), pp. 3189–3204. Available at: https://doi.org/10.1016/j.jmrt.2024.09.224.

[14] Steinfelder, C., Rempel, D. and Brosius, A. (2024) 'Influence of the material properties on the clinching process and the resulting load-bearing capacity of the joint', *Journal of Advanced Joining Processes*, 10(February), p. 100263. Available at: https://doi.org/10.1016/j.jajp.2024.100263.

[15] Valikhani, M. *et al.* (2024) 'Bayesian finite element model inversion of offshore wind turbine structures for joint parameter-load estimation', *Ocean Engineering*, 313(P3), p. 119458. Available at: https://doi.org/10.1016/j.oceaneng.2024.119458.

Citation of this Article:

Djoeli Satrijo, Ojo Kurdi, Toni Prahasto, Sabrina Rizky Mulyana, & Ian Yulianti. (2024). Fatigue and Damage Tolerance Analysis on Center Wing N-XXX Aircraft Using Software. *International Research Journal of Innovations in Engineering and Technology - IRJIET*, 8(11), 122-127. Article DOI https://doi.org/10.47001/IRJIET/2024.811011

****